Theoretical evidence for the correlation between hole density and T_c in high-T_c Tl-based superconductors

Bal K. Agrawal, Sudhir Kumar, S. Agrawal, and P. S. Yadav
Department of Physics, University of Allahabad, Allahabad 211 002, India
(Received 16 May 1991; revised manuscript received 10 November 1992)

A tight-binding calculation has been performed for determining the electronic structure of the Tl-monolayer superconducting systems $TlBa_2Ca_{n-1}Cu_nO_{2n+3}$, for $n=1$–6 and the Tl-bilayer systems $Tl_2Ba_2Ca_{n-1}Cu_nO_{2n+4}$, for $n=1$–4. In the Tl-monolayer systems, the antibonding Tl(6s)-$O_3(p_z)$ band appears well above the hybridized $Cu(d_{x^2-y^2})$-$O_1(p_{x,y})$ bands throughout the Brillouin zone and remains unoccupied. On the other hand, in the Tl-bilayer systems, one of the antibonding Tl(6s)-$O_3(p_z)$ band appears well above the hybridized $Cu(d_{x^2-y^2})$-$O_1(p_{x,y})$ bands throughout the whole Brillouin zone and is unoccupied. However, some parts of the other Tl(6s)-$O_3(p_z)$ antibonding band either touch the Fermi surface or cross it. The valences of the atoms lying in the Ba-O layers and in the Ca layer are quite similar in both the Tl-monolayer and -bilayer systems. In the Tl-monolayer systems, the number of electrons residing on one Cu atom increases with the number of the CuO_2 layers in contrast to the Tl-bilayer systems, where the electrons on the Cu atoms are larger and do not change with the number of Cu-O_2 layers. On the other hand, the number of electrons on O atoms of the CuO_2 layer are similar in both the systems. The Tl valences in the Tl-monolayer and -bilayer systems are seen to be around 2.4 and 1.3, respectively, which indicates a bias towards the respective occurrence of the nearly trivalent Tl^{+3} and the monovalent Tl^+ ions in the Tl-monolayer and -bilayer systems. The number of electrons in the O atoms lying in the Tl-layers is seen to be larger in the monolayer systems as compared to those in the bilayer systems. In both the systems, the hole density on the Cu-d orbitals is seen to be larger than the O-p orbitals lying in the CuO_2 layers. The hole density per unit cell at the Cu atom increases with the number of CuO_2 layers, a result that is in conformity with the observed enhancement in the transition temperatures T_c in these phases. The calculated density of states for the $Tl_2Ba_2Ca_2Cu_3O_{10}$ is in very good agreement with the only available x-ray photoemission spectroscopy and inverse-photoemission-spectroscopy data in terms of the number of location of peaks.

I. INTRODUCTION

In the recently discovered high-T_c oxide superconductors, the highest T_c has been achieved in the Tl-based perovskites like the homologous series $TlBa_2Ca_{n-1}Cu_nO_{2n+3}$ for $n=4$ ($T=122$ K) or the series $Tl_2Ba_2Ca_{n-1}Cu_nO_{2n+4}$ for $n=3$ ($T_c=125$ K). These compounds have thus drawn great attention towards the understanding of the mechanism responsible for high-T_c superconductivity. In the Tl-Ba-Ca-Cu-O superconducting systems, at least eight structural phases are known. These phases can be divided into two series: $TlBa_2Ca_{n-1}Cu_nO_{2n+3}$ ($n=1,6$) and $Tl_2Ba_2Ca_{n-1}Cu_nO_{2n+4}$ ($n=1,4$). There are uncertainties about the exact site occupancies, oxygen stoichiometries, and Tl and Cu valences. Also, there evidence of occurrence of Tl-Ca disorder, additional or deficient Cu-O_2 layers and distortion within the Tl-O layers in some phases.[1]

In a distinct series of Tl-monolayer phases, namely, $TlBa_2Ca_{n-1}Cu_nO_{2n+3}$ ($n=1,6$), the second Tl-O layer present in the analogous series of $Tl_2Ba_2Ca_{n-1}Cu_nO_{2n+4}$ is absent and the Bravais lattice changes from the body-centered-cubic to the simple tetragonal[2–5] one.

In the Tl-monolayer series, the $n=1$ phase was found to be nonsuperconducting. However, recently its Ba-La alloys $TlBa_{2-x}La_xCuO_5$ have been seen to be superconducting with a maximum values of $T_c\sim 40$ K near $x\sim 0.8$.[6,7] For the other pure Tl-monolayer phases, the values of T_c increases to $n=4$ and decreases thereafter for the $n=5$ phase, i.e., 80 K for $n=2$, 110 K for $n=3$, and 122 K for $n=4$. However, T_c decreases slightly for the $n=5$ phase, $TlBa_2Ca_4Cu_5O_{13}$ to 110 K. Superconductivity has also been observed in the $Tl_{1-x}SrLaCu_{1+x}O_5$ systems.[8] Also, superconductivity up to $T_c=120$ K has been measured in 50-50 % Tl-Pb alloys $(Tl,Pb)Sr_2Ca_{n-1}Cu_nO_{2n+3}$ (Ref. 9) and $(Tl,Pb)Ba_2Ca_{n-1}Cu_nO_{2n+3}$ (Ref. 10).

The basic difference between the Tl-monolayer and bilayer phases is that in the latter one observes two pairs of the strongly bonding-antibonding Tl(s)-O(p_z) bands out of which the lower of the two antibonding $(sp\sigma)^*$ bonds is partially occupied by the valence electrons. In the Tl-bilayer cuprates, it may result in the occurrence of the monovalent Tl ion (Tl^+). Also, it suggests the valences of oxygen atoms lying in the Ba as well as in the Tl planes to be -1 and not the expected -2. However, recently NMR studies performed on Tl-bilayer compounds ($n=3$) have suggested[11] the occurrence of the trivalent Tl ions. The present investigations for the Tl-bilayer sys-

tems suggest a valency of Tl slightly higher than 1 (~ 1.33). On the other hand, in the Tl-monolayer systems $TlBa_2Ca_{n-1}Cu_nO_{2n+3}$ ($n=1,6$), one expects a single bonding-antibonding $(sp\sigma)$-$(sp\sigma)^*$ pair. The present results reveal that the single antibonding $(sp\sigma)^*$ is quite a bit above the Fermi level (>1.0 eV) and is unoccupied. It results in the approximate loss of one more electron from the Tl atom resulting in the occurrence of the more ionic Tl^{+3} ion.

A knowledge of the electronic structure of these systems is an important first step towards the understanding of its normal-state properties from which an understanding of the mechanisms of superconductivity will emerge. Earlier, a number of efforts in this direction have been made by several groups.[12–14]

Recently, we have been involved in a detailed and comprehensive study of the electronic and vibrational excitations of the Tl-monolayer and bilayer systems.[15] The results for the dispersion curves and the density of states of the phonons have been reported elsewhere.[16,17] The study of the systems containing substitutional atoms would be presented in another paper.[18]

In the present article, we have studied the electronic structure of the Tl-monolayer systems $TlBa_2Ca_{n-1}Cu_nO_{2n+3}$ (for $n=1-6$) and the Tl-bilayer systems $Tl_2Ba_2Ca_{n-1}Cu_nO_{2n+4}$ ($n=1-4$) and the results are then employed for finding correlations, if any exist, between the hole concentration and T_c. Section II contains a brief summary of the method and details of the calculation and the results for the eight phases. A brief summary and the conclusions are included in Sec. III.

II. CALCULATION AND RESULTS

The Tl-bilayer systems possess body-centered-tetragonal crystal structures with space group $I4/mmm$, whereas the Tl-monolayer systems possess the simple tetragonal structure with space group $P4/mmm$. The value of the lattice parameter a in the plane changes slightly (by $\sim 0.4\%$) on going from $n=1$ to $n=3$ for the Tl-bilayer compounds, we assume it to be the same for all the different phases as $a=3.855$ Å. For the Tl-monolayer systems where n is even, the different layers containing Ca, Cu-O, Ba-O, and Tl-O atoms are positioned along the c axis as (0, c_1, c_2, and c_3) with values equal to 1.60, 2.0, and 2.75 Å, respectively, whereas, for the corresponding Tl-bilayer systems, the values for c_1, c_2, c_3 and c_4 are 1.60, 2.714, 2.123, and 2.0 Å, respectively.

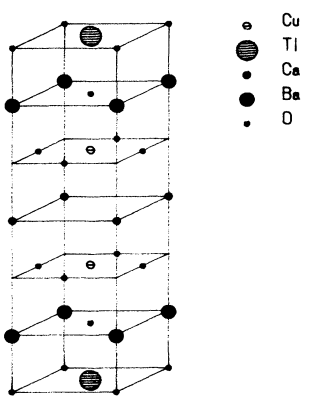

FIG. 1. Primitive simple-tetragonal unit cell for $TlBa_2CaCu_2O_7$. Oxygen atoms in the Cu, Ba, and Tl planes are denoted by O(1), [or O(2)], O(3), and O(4), respectively.

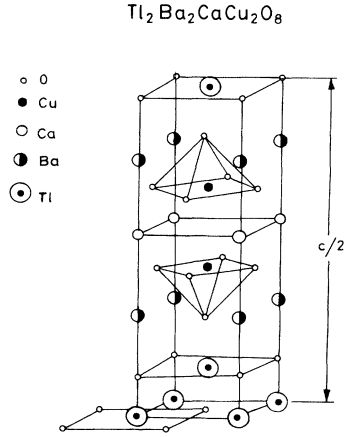

FIG. 2. Primitive body-centered-tetragonal unit cell for $Tl_2Ba_2CaCu_2O_8$. Oxygen atoms in the Cu, Ba, and Tl planes are denoted by O(1), [or O(2)], O(3), and O(4), respectively.

The atoms in one formula unit for the double Cu-O_2 layer phase, $TlBa_2CaCu_2O_7$ are shown in the Fig. 1. The coordinates are Ca $(\pm\frac{1}{2},\pm\frac{1}{2},0)$ Cu $(0,0,c_1)$, O_1 $\mp(\frac{1}{2},0,c_1)$, O_2 $\mp(0,\frac{1}{2},c_1)$, Ba $\pm(\frac{1}{2},\frac{1}{2},\mp c_2)$, O_3 $\mp(0,0,c_2)$, O_4 $\pm(\frac{1}{2},\frac{1}{2},c_3)$ and Tl $(0,0,c_3)$. In contrast to the bilayer phases, where one unit cell possesses two formula units—one displaced with respect to other by $(\frac{1}{2},\frac{1}{2},\frac{1}{2})$, the unit cell of the single Tl-O layer phases $TlBa_2Ca_{n-1}Cu_nO_{2n+3}$ contains only one formula unit.

The atoms in one formula unit for the double Cu-O_2 layer phase $Tl_2Ba_2CaCu_2O_8$ are shown in Fig. 2. The coordinates are Ca $\pm(\frac{1}{2},\frac{1}{2},0)$, Cu $\pm(0,0,c_1)$, O_1 $\mp(\frac{1}{2},0,c_1)$, O_2 $\mp(0,\frac{1}{2},c_1)$, Ba $\pm(\frac{1}{2},\frac{1}{2},c_2)$, O_3 $\mp(0,0,c_2)$, O_4 $\mp(\frac{1}{2},\frac{1}{2},c_3)$, and Tl $\pm(0,0,c_3)$.

A tight-binding approximation considering all the nearest-neighboring interaction integrals has been used in the calculation. For the Tl-monolayer systems, we consider a set of (s,p) orbitals for O and Ca, (d,s) orbitals for

TABLE I. Self-site orbital energies in eV.

Atom	E_s	E_p	E_d
Cu	−12.00		−14.00
O	−29.00	−14.00	
Ca	−5.42	−33.76	
Tl	−9.90[a]	−4.60[a]	−24.00
Ba	−4.50	−22.85	−6.60

[a]For the Tl-bilayer systems, $Tl_2Ba_2Ca_{n-1}Cu_nO_{2n+4}$, the values have been shifted by 3.29 eV towards the low-energy side.

TABLE II. Interaction matrix elements for the Tl-monolayer $TlBa_2Ca_{n-1}Cu_nO_{2n+3}$ systems in eV.

Bond	Bond length (Å)	$ss\sigma$	$sp\sigma$	$pp\sigma$	$pp\pi$	$sd\sigma$	$pd\sigma$	$pd\pi$
Cu-O_1 (O_2)	1.928	−2.26	1.85	0.00	0.00	−1.14	−1.77	0.99
Cu-O_3	2.000	−2.10	1.71	0.00	0.00	−1.00	−1.56	0.87
Ba-O_1 (O_2)	2.726	−1.13	0.92	1.54	−0.62	−0.74	−1.15	0.65
Ba-O_3	2.750	−1.11	0.91	1.51	−0.60	−0.72	−1.12	0.63
Tl-O_3	2.726	−1.13	0.92	1.54	−0.62	−0.36	−0.57	0.32
Tl-O_4	2.750	−1.11	0.91	1.51	−0.60	−0.35	−0.55	0.31
Ca-O_3	2.505	−1.34	1.09	1.82	−0.73	0.00	0.00	0.00

Cu, and (d,s,p) orbitals for both the Tl and Ba atoms. However, in order to reduce the sizes of secular matrices in the Tl-bilayer systems, we restrict ourselves to the consideration of the p orbitals for O, s orbitals for Ca and Ba atoms, d and s orbitals for Cu, and a set of (s,p) orbitals for Tl. However, we have checked the results by performing calculations for the Tl-bilayer systems after employing the larger basis similar to that used for the Tl-monolayer systems. The results for the two basis sets are much the same, and the use of a smaller basis does not at all affect the results. For all the atoms, we have employed the atomic energy values[19] for the self-site interaction integral values for the various orbitals except for the d orbital of Cu, where a shift towards the higher-energy side by 2.1 eV has been made. This has been found to be necessary to obtain hybridization of the Cu-d orbitals with the O-p orbitals bringing them to the same energy value, −14.0 eV.

For the Tl orbitals, in the case of Tl-monolayer systems, atomic values have been chosen.[19] The Tl-s states were seen to appear well above the Fermi level. However, for the Tl-bilayer systems, the linear augmented plane wave (LAPW) calculations reveal that the Tl-s states either touch or cross the Fermi level. We, therefore, have shifted the Tl-orbital energies from their atomic values by a value 3.29 eV towards the low-energy side. The values of the matrix elements used are presented in Table I.

The interatomic interaction integrals are determined by using the simple expressions by Harrison:[20]

$$V_{ll'm}=\eta_{ll'm}\hbar^2/(m_e d)^2 \quad (l,l'=s \text{ or } p)$$

and

$$V_{ldm}=\eta_{ldm}\hbar^2 r_d^{3/2}/(m_e d^{7/2}) \quad (l=s \text{ or } p)\ ,$$

where $\hbar$ is Planck's constant, m_e is the electron mass, and d denotes the interatomic separation. Here η's have the values

$$\begin{aligned} &\eta_{ss\sigma}=-1.1\ , \quad \eta_{sp\sigma}=0.9\ , \\ &\eta_{sd\sigma}=-1.6\ , \quad \eta_{pd\sigma}=-2.5\ , \\ &\eta_{pp\sigma}=1.5, \quad \eta_{pp\pi}=-0.6 \end{aligned} \tag{1}$$

and

$$\eta_{pd\pi}=1.4\ .$$

Here r_d stands for the size of the d-orbital interaction and is equal to 0.95 Å for Cu and 1.6 Å for the other metal ions. The values of the various interaction integrals used are included in Tables II and III for the Tl-monolayer and -bilayer systems, respectively.

The computed electron energy dispersion curves for the five Tl-monolayer phases ($n=1,5$) along some symmetry directions in the simple tetragonal Brillouin zone have been depicted in Figs. 3–7. The symmetry points for the space group P_4/mmm are $\Gamma(0,0,0)$, $X(1,0,0,)$, $M(1,1,0)$, $\Gamma(0,0,0)$, $Z(0,0,1)$ $R(1,1,1)$, $A(1,0,1)$, and $Z(0,0,1)$. In these figures, we have also included the results of a plane shifted in the c direction in order to see the changes in dispersion along the c axis.

The computed electron energy dispersion curves for the three phases ($n=1-3$) of the Tl-bilayer systems along some symmetry directions in the body-centered-tetragonal Brillouin zone have been depicted in Figs.

TABLE III. Interaction matrix elements for the Tl-bilayer systems, $Tl_2Ba_2Ca_{n-1}Cu_nO_{2n+4}$ in eV.

Bond	Bond length (Å)	$sp\sigma$	$pp\sigma$	$pp\pi$	$sd\sigma$	$pd\sigma$	$pd\pi$
Cu-O_1 (O_2)	1.928				−1.14	−1.77	0.99
Cu-O_3	2.714				−0.34	−0.54	0.30
Ba-O_1 (O_2)	2.818	0.86					
Ba-O_3	2.836	0.85					
Tl-O_3	2.123	1.52	2.54	−1.01			
$(Tl\text{-}O_4)_{x,y}$	2.726	0.92	1.54	−0.62			
$(Tl\text{-}O_4)_{+z}$	2.000	1.71	2.86	−1.14			
Ca-O_3	2.505	1.09					

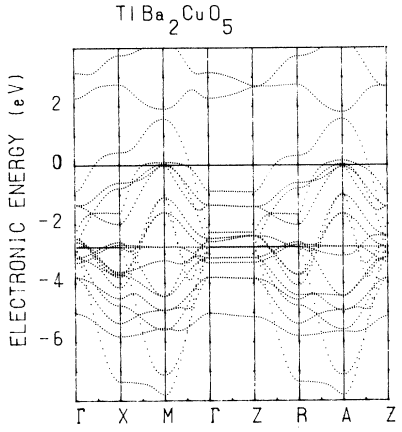

FIG. 3. Electron energy dispersion curves for $TlBa_2CuO_5$ in two planes normal to the c axis.

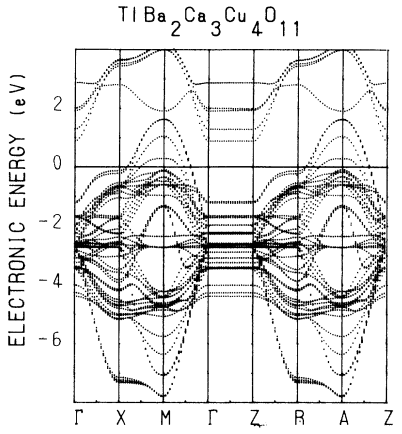

FIG. 6. Same as Fig. 3 except for $TlBa_2Ca_3Cu_4O_{11}$.

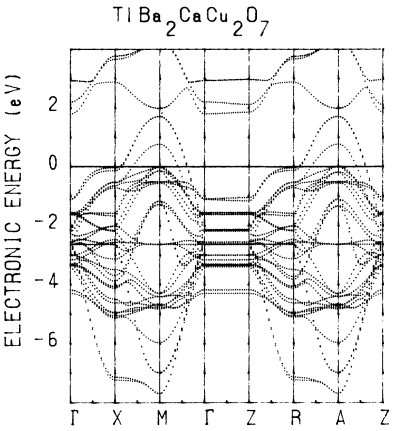

FIG. 4. Same as Fig. 3 except for $TlBa_2CaCu_2O_7$.

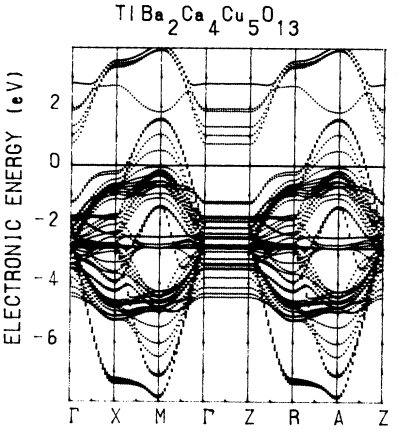

FIG. 7. Same as Fig. 3 except for $TlBa_2Ca_4Cu_5O_{13}$.

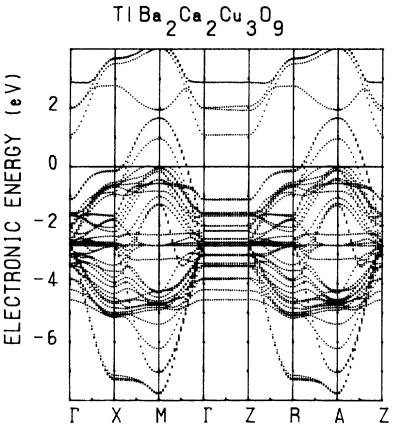

FIG. 5. Same as Fig. 3 except for $TlBa_2Ca_2Cu_3O_9$.

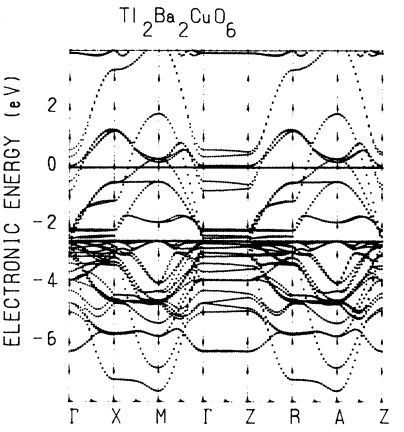

FIG. 8. Same as Fig. 3 except for $Tl_2Ba_2CuO_6$.

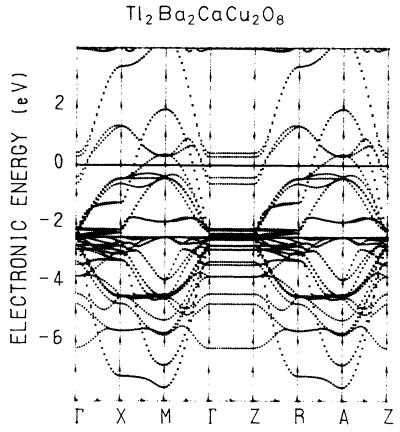

FIG. 9. Same as Fig. 3 except for $Tl_2Ba_2CaCu_2O_8$.

8–10. The symmetry points for the space group $I4/mmm$ are $\Gamma(0,0,0,)$, $X(1,0,0)$, $M(1,1,0)$, $\Gamma(0,0,0)$, $Z(0,0,1)$, $R(1,1,1)$, $A(1,0,1)$, and $Z(0,0,1)$.

The important bands lying in the neighborhood of the Fermi level arise mainly from Cu($3d$), O($2p$), and Tl($6s$) states and lie in the approximate energy range $-7.0-+3.0$ eV. The uppermost bands above $+3.0$ eV originate from the Ba($5d$)- and Tl-(p)-like states.

There are Cu($d_{x^2-y^2}$)-O($p_{x,y}$) antibonding states, which cross the Fermi surface in most of the volume of the Brillouin zone barring the Γ-symmetry region. This band is exactly half filled and is expected to make the phase both antiferromagnetic and insulating. In order to make the phase metallic and superconducting, extra carriers (electrons or holes) have to be introduced into the CuO_2 planes by doping. The maximum dispersion is seen for the Cu($d_{x^2-y^2}$)-O_1($p_{x,y}$) [Cu($d_{x^2-y^2}$)-O_2($p_{x,y}$)] bands whose width is more than 4 eV. The other Cu(d) bands hybridized with the O(p) orbitals either touch the Fermi surface or just cross it. These bands are degenerate at the more symmetric k points such as Γ(000) or X(100)

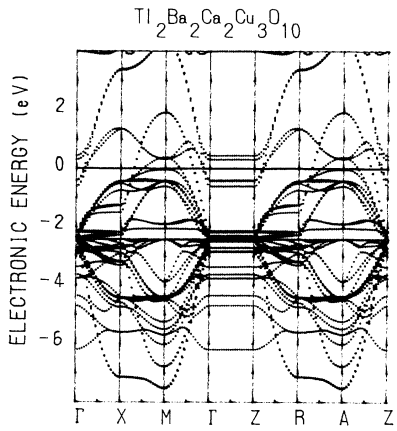

FIG. 10. Same as Fig. 3 except for $Tl_2Ba_2Ca_2Cu_3O_{10}$.

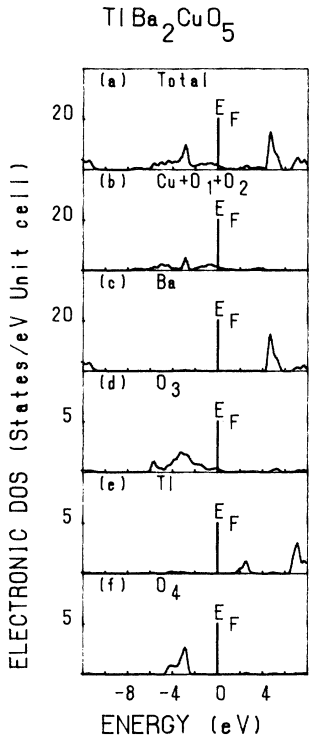

FIG. 11. Projected electron densities of states of the orbitals at the various atoms in $TlBa_2CuO_5$. (a) Total of all orbitals of all atoms. (b) Sum of the local densities of (s,d) orbitals of Cu and (s,p) orbitals of O_1 and O_2 atoms. (c) Sum of the local densities of (s,p,d) orbitals of Ba. (d) Sum of the local densities of (s,p) orbitals of O_3 lying in the Ba plane. (e) Sum of the local densities of (s,p,d) orbitals of Tl. (f) Sum of the local densities of (s,p) orbitals of O_4 lying in the Tl plane.

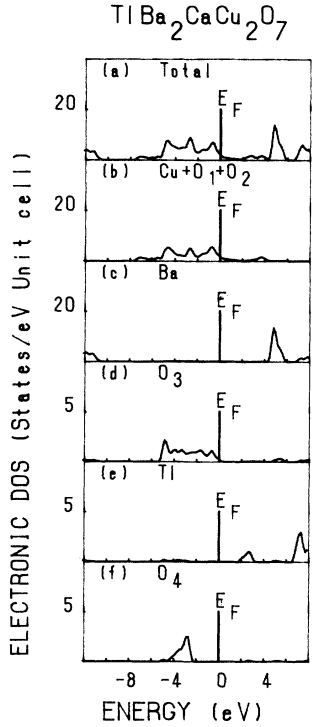

FIG. 12. Same as Fig. 11 except for $TlBa_2CaCu_2O_7$.

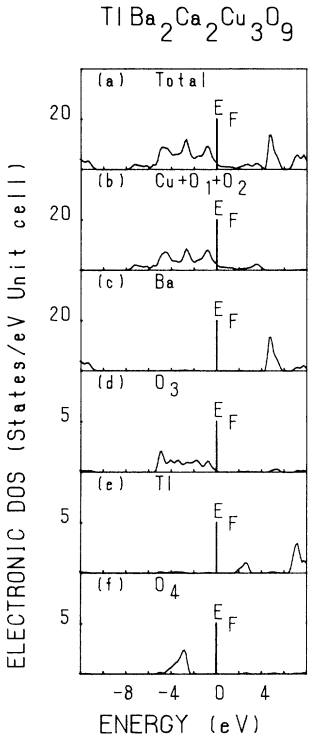

FIG. 13. Same as Fig. 11 except for $TlBa_2Ca_2Cu_3O_9$.

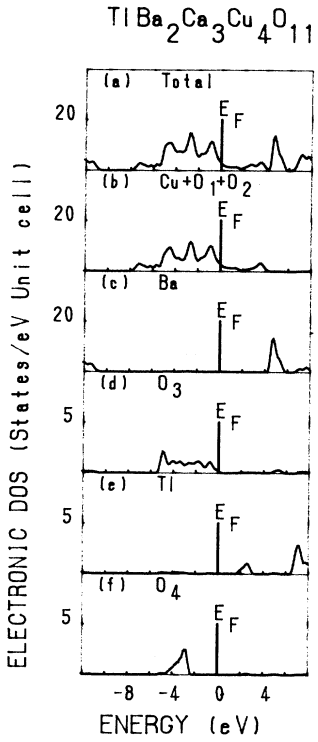

FIG. 14. Same as Fig. 11 except for $TlBa_2Ca_2Cu_4O_{11}$.

$[D(100)]$. However, these degeneracies are removed as one moves away from these symmetric points or directions.

In the Tl-monolayer systems, the Tl($6s$)-$O_3(p_z)$ antibonding band appears in the energy region above the mixed Cu(d)-O(p) states throughout the whole Brillouin zone and remains totally unfilled for all the phases. This behavior is totally different from that observed in the Tl-bilayer systems, where one of the Tl-O $sp\sigma^*$ bands lies below the Fermi level and is partially occupied. Almost all the bands in the various phases show a two-dimensional behavior except for the single CuO_2 layer phase, $TlBa_2CuO_5$, where these bands show some dispersion along the c axis. The number of the antibonding Cu(d)-O(p) bands crossing the Fermi surface increase with the number of CuO_2 layers. The two-dimensional behavior of the bands approaches towards more perfection with the inclusion of more and more CuO_2 layers in these Tl-based phases. When the present work was in final preparation we came across the results of a local-density self-consistent calculation[21] for the single CuO_2 layer system, $TlBa_2CuO_5$. The present results are in agreement with them.

For the Tl-monolayer systems, the density of states along with their projected values at the various atoms, have been calculated for a mesh of variable number of points in $\frac{1}{16}$ of the irreducible volume of the simple tetragonal Brillouin zone for all the systems. The whole energy range was divided into 270 parts for the calculation of density of states. In the calculation, no broadening has been incorporated. The projected densities or the local densities have been calculated by employing the relation,

$$N_i(E)=\sum_{\alpha}|\psi_i^{\alpha}(E)|^2N(E)\ , \tag{2}$$

TABLE IV. Density of states for all atoms of each type per eV per unit cell at Fermi level $N(E_F)$ at various atoms $TlBa_2Ca_{n-1}Cu_nO_{2n+3}$ systems.

Orbital	$n=1$	$n=2$	$n=3$	$n=4$	$n=5$	$n=6$
Cu-d	0.9315	1.0938	1.3587	1.4835	1.6002	1.162
O_1(Cu)-p	1.1936	1.6648	1.1736	1.3480	1.5035	2.630
O_3(Ba)-p	0.4096	0.2712	0.2296	0.1922	0.1626	0.069
Total[a]	1.8944	2.415	3.015	3.312	3.571	3.964

[a]The total DOS includes contributions from the other atoms of the unit cell.

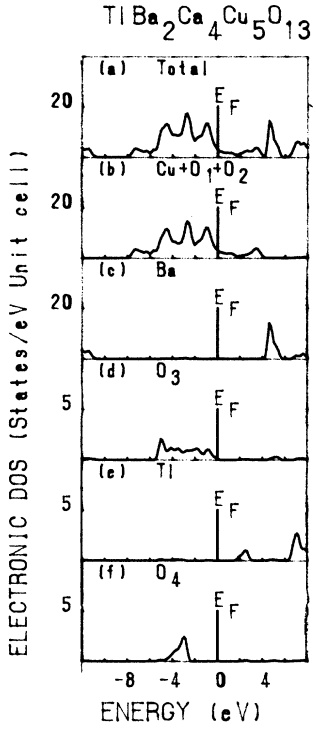

FIG. 15. Same as Fig. 11 except for $TlBa_2Ca_4Cu_5O_{13}$.

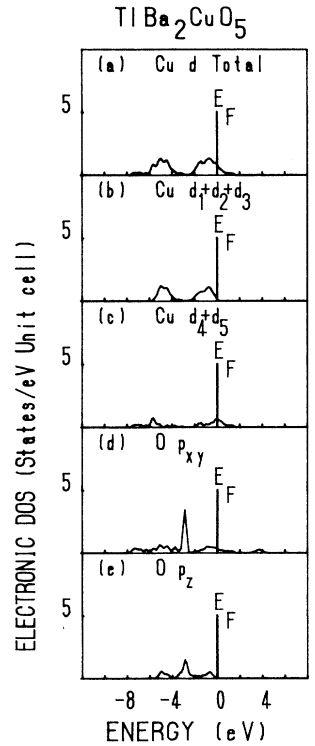

FIG. 16. Projected electron densities of states of the orbitals of various atoms in $TlBa_2CuO_5$. (a) Sum of the local densities of all the d orbitals of the Cu atom. (b) Sum of the local densities of $(d_1+d_2+d_3)$ orbitals of Cu. (c) Sum of the local densities of (d_4+d_5) orbitals of the Cu atom. (d) Sum of the local densities of (p_x+p_y) orbitals of O_1 and O_2 lying in the Cu plane. (e) Sum of the local densities of (p_z) orbitals of O_1 and O_2 lying in the Cu plane.

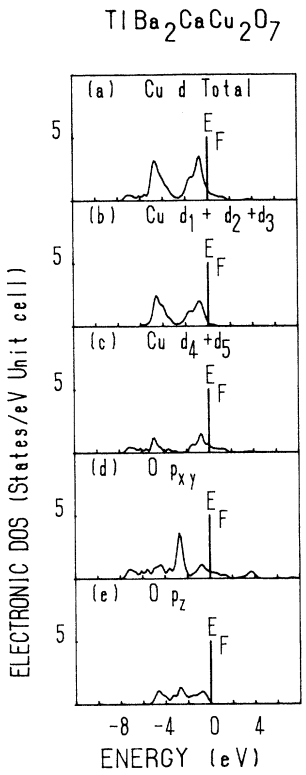

FIG. 17. Same as Fig. 16 except for $TlBa_2CaCu_2O_7$.

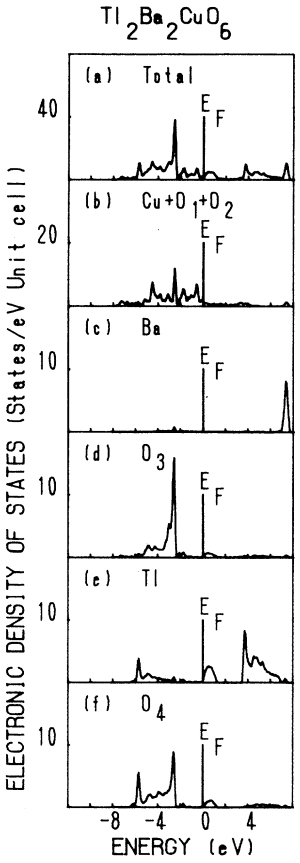

FIG. 18. Same as Fig. 11 except for $Tl_2Ba_2CuO_6$.

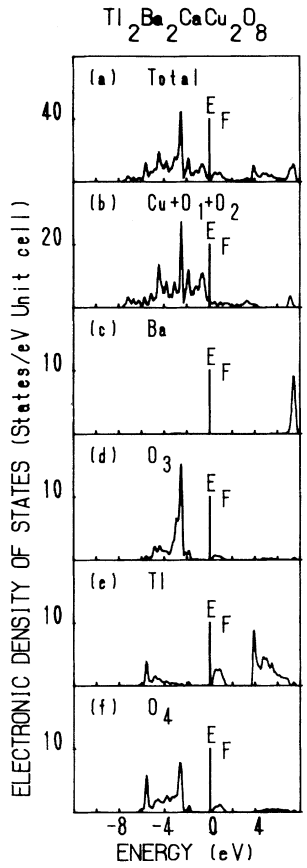

FIG. 19. Same as Fig. 11 except for $Tl_2Ba_2CaCu_2O_8$.

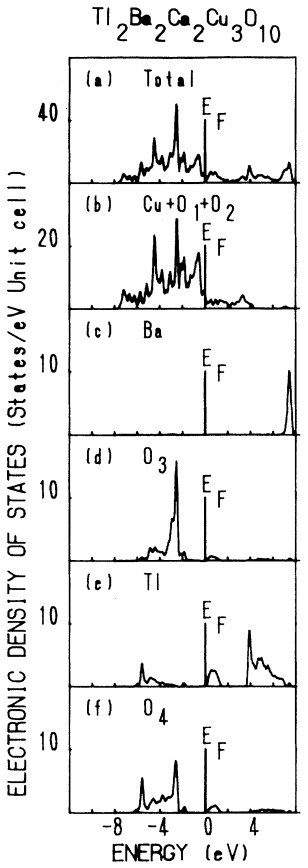

FIG. 20. Same as Fig. 11 except for $Tl_2Ba_2Ca_2Cu_3O_{10}$.

where $N_i(E)$ is the local density at atom i out of the total density of states $N(E)$ and $\psi_i^\alpha(E)$ is the eigenvector belonging to the orbital α at site i for the energy eigenvalue E.

The local densities of states for the various phases $TlBa_2Ca_{n-1}Cu_nO_{2n+3}$ ($n=1,6$) have been depicted in Figs. 11–15. One observes from panels (e) and (f) of Figs. 11–15, where the densities at Tl and inplane O atoms have been depicted, that the TlO layer is insulating. The bonding-antibonding Tl(s)-O(p) bands are quite separated, and the density of states vanishes from both the Tl and O atoms at the Fermi level. The same is also true for the Ba-O layer [see panels (c) and (d) for their local densities].

On the other hand, the Cu-O_2 layers reveal a metallic behavior. There appear appreciable local densities of states on both the O and Cu atoms as shown in panels (a) and (b) of Figs. 16 and 17.

In order to see the behavior of the Cu-O_2 layer within the layer and normal to the layer direction, we have separated the two contributions and have shown them for the first two members of the family, $TlBa_2CuO_5$ and $TlBa_2CaCu_2O_7$ in Figs. 16 and 17. The five d orbitals have the usual notation: $d_1=d_{xy}$, $d_2=d_{yz}$, $d_3=d_{zx}$, $d_4=d_{x^2-y^2}$ and $d_5=d_{3z^2-r^2}$. One may easily note the metallic behavior of the CuO_2 layer within the plane and an insulating behavior along the c direction.

The contributions of the TlO and BaO layers towards the total density of states remain unaltered with an increase in the Cu-O_2 layers, as is evident from panels (e) and (f) of the Figs. 11–15. The corresponding peaks of these layers also do not shift with the change in the number of CuO_2 layers.

The contributions of the different orbitals to the density of states at the Fermi level $N(E_F)$ for the different phases ($n=1-6$) are shown in Table IV. The main contributions arise from the Cu(d) and O_1(p) orbitals. The

TABLE V. Density of states for all atoms of each type at Fermi level $N(E_F)$ at various atoms per unit cell for $Tl_2Ba_2Ca_{n-1}Cu_nO_{2n+4}$ systems ($n=1$ to 4).

Orbital	$n=1$	$n=2$	$n=3$	$n=4$
Cu-d	0.848	0.710	1.566	1.910
O(Cu)-p	0.875	0.760	1.564	1.920
O_3-p	0.062	0.014	0.017	0.017
Total[a]	1.94	1.986	2.18	4.52

[a]The total DOS includes contributions from the other atoms of the the unit cell.

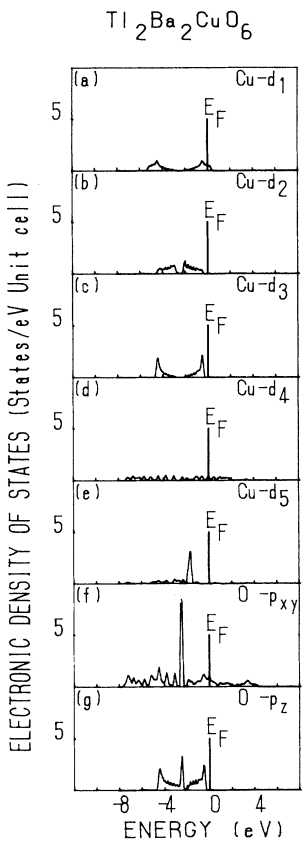

FIG. 21. Projected DOS of Cu-*d* and O-*b* orbitals for $Tl_2Ba_2CuO_6$.

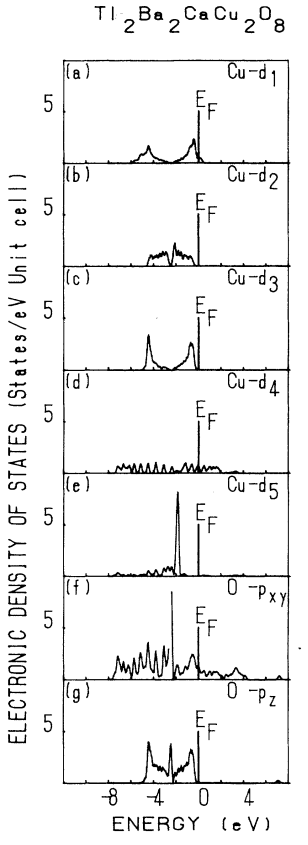

FIG. 22. Same as Fig. 21 except for $Tl_2Ba_2CaCu_2O_8$.

TABLE VI. Values of Δn for the various atoms in the six $TlBa_2Ca_{n-1}Cu_nO_{2n+3}$ systems for $n=1-6$.

System	Cu	O(Cu)	Ba	O(Ba)	Tl	O(Tl)	Ca
$TlBa_2CuO_2$	1.37	−1.42	1.60	−1.60	2.40	−1.44	
$TlBa_2CaCu_2O_2$	1.07	−1.28	1.60	−1.60	2.37	−1.44	1.79
$TlBa_2Ca_2Cu_3O_2$	0.96	−1.28	1.60	−1.60	2.37	−1.44	1.79
$TlBa_2Ca_3Cu_4O_2$	0.91	−1.28	1.60	−1.60	2.37	−1.45	1.79
$TlBa_2Ca_4Cu_5O_2$	0.88	−1.28	1.60	−1.60	2.37	−1.45	1.79
$TlBa_2Ca_5Cu_6O_2$	0.86	−1.27	1.59	−1.59	2.36	−1.45	1.79

TABLE VII. Values of Δn for the various atoms in $Tl_2Ba_2Ca_{n-1}Cu_nO_{2n+4}$ ($n=1-4$).

System	Valency (Δn)						
	Cu	O_1	Ba	O_3	Tl	O_4	Ca
$Tl_2Ba_2CuO_2$	0.81	−1.35	1.93	−1.39	1.33	−0.92	
$Tl_2Ba_2CaCu_2O_2$	0.77	−1.30	1.93	−1.39	1.33	−0.92	1.79
$Tl_2Ba_2Ca_2Cu_3O_2$	0.75	−1.29	1.93	−1.39	1.33	−0.92	1.80
$Tl_2Ba_2Ca_3Cu_4O_2$	0.74	−1.28	1.93	−1.39	1.33	−0.92	1.80

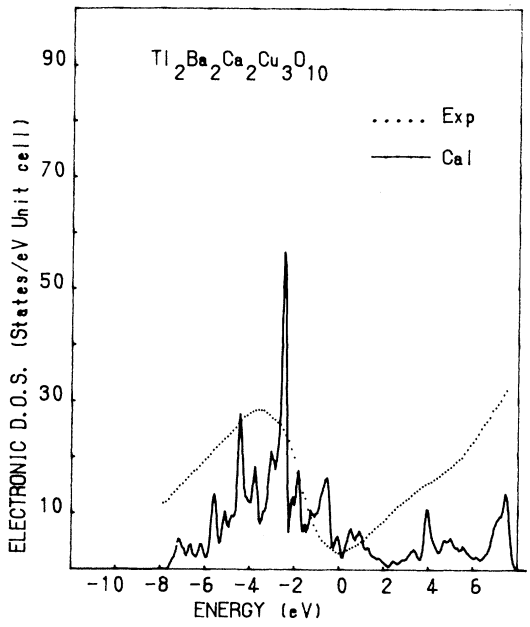

FIG. 23. Comparison of the calculated total electronic DOS with the XPS and IPES data of Meyer *et al.* (Ref. 22) for $Tl_2Ba_2Ca_2Cu_3O_{10}$.

local density of states at oxygen atoms lying in the CuO_2 layers increases about fourfold going from the $n=1$ to the $n=6$ phase. The total density at E_F, $N(E_F)$, increases from 1.89 to 3.96 (states eV^{-1}) unit cell in the six Tl-monolayer phases.

For the Tl-bilayer systems, the density of states (DOS) along with their projected values at the various atoms have been calculated for a mesh of 408 points in $\frac{1}{16}$ of the irreducible volume of the Brillouin zone. The whole energy range was divided into 270 parts for the calculation of density of states.

The local densities of states for the various phases of $Tl_2Ba_2Ca_{n-1}Cu_nO_{2n+4}$ ($n=1-4$) have been depicted in Figs. 18–22. One observes from panels (e) and (f) of Figs. 18–20, where the densities at the Tl and the in-plane O atom have been plotted that the Tl-O layer is nearly insulating. The Tl(s)-O(p) bonding and antibonding bands are separated and the densities of states are quite small both on the Tl and O atoms at the Fermi level. The same is also true for the Ba-O layer [see panels (c) and (d) for their local densities].

The contributions of the various Cu-d orbitals, d_1 (xy), d_2 (yz), d_3 (zx), d_4 (x^2-y^2), and d_5 ($3z^2-r^2$) for the first two members of the family of the Tl-bilayer systems, are shown in Figs. 21 and 22. One again may note that the DOS at Fermi level for the d_2-, d_3-, and d_5-like orbitals of Cu and the p_z orbitals of O vanish. Thus, all the orbitals containing a z-component reveal no density at E_F. On the other hand, the Cu-d_1, d_4 and O_{xy} orbitals have nonvanishing values at E_F, revealing the metallic behavior of the Cu-O_2 layers.

In Fig. 23, we have compared the calculated DOS with the photoemission data[22] available for the $Tl_2Ba_2Ca_2Cu_3O_{10}$ system. A broad experimental peak appearing in the valence states region of x-ray photoemission spectroscopy (XPS) data is in very close agreement with the calculated peak. It should be noted that in the calculation we have not used any broadening in the states. Similarly, the two shoulders in the conduction-band region in the IPES data appearing at ~ 3 and ~ 7 eV are in excellent agreement with the calculated peaks at ~ 4 and ~ 7.4 eV.

Similar to the Tl-monolayer systems, the contributions of the Tl-O and Ba-O layers towards the total density of states remain unaltered with an increase in the Cu-O_2 layers. Also, the corresponding peaks of these layers do not shift with the change in the number of Cu-O_2 layers. The density of states at the Fermi level for the different phases ($n=1-4$) are shown in Table V. The main contributions that arise from the Cu(d) and $O_1(p)$ orbitals in the Tl-bilayer systems are, in general, are compared to those seen in the Tl-monolayer systems, and are also nearly equal. $N(E_F)$ for the two or three CuO_2 layer systems increases to two or three times its value for the one CuO_2 system. The total density at E_F, $N(E_F)$, increases from 1.99 to 4.52 (states eV^{-1}) unit cell.

The electron occupancy n_i of the various states at site i occupied by an atom of atomic number Z is determined by taking a weighted average over the whole Brillouin zone using the relation

$$n_i = Z \sum_{E \le E_F} \sum_{\alpha} |\psi_i^{\alpha}(E)|^2 . \tag{3}$$

We define Δn_i as the difference between the number of valence electrons on the isolated atom and currently determined occupancy n_i. In fact, Δn_i denotes the number of electrons lost or gained by the atom. The values of Δn_i for the Tl-monolayer and the Tl-bilayer systems are shown in Tables VI and VII, respectively.

Here, all the bonds retain some covalent character. Thus, Δn_i may be somewhat smaller as compared with the traditional formal valence discussed in the chemistry as is evident from Tables VI and VII. The actual valence of atom i may be some multiple of Δn_i. One can, howev-

TABLE VIII. Hole concentrations in different orbitals per unit cell in $TlBa_2Ca_{n-1}Cu_nO_{2n+3}$ phases.

Atomic orbital	$n=1$	$n=2$	$n=3$	$n=4$	$n=5$	$n=6$
Cu-d*	1.028	1.4568	1.9400	2.6334	3.0277	3.992
O_1- and O_2	0.607	1.3684	1.9447	4.898	6.0640	7.296
O_3-p	0.099	0.0038	0.0024	0.002	0.0016	

TABLE IX. Hole concentrations per unit cell in different orbitals in $Tl_2Ba_2Ca_{n-1}Cu_nO_{2n+4}$ phases for $n=1-4$.

Atomic orbital	$n=1$	$n=2$	$n=3$	$n=4$
Cu-d[a]	1.5504	2.9824	4.2690	5.1184
O_1- and O_2-p	2.6332	5.1768	7.7248	7.9464

[a]Hole concentration is for all the Cu atoms in the unit cell.

er, note trends of the changes in Δn_i with increase in the number of CuO_2 layers.

For the Tl-monolayer systems, striking changes are seen for Cu, where the valence decreases with the number of CuO_2 layers. Thus, the extra CuO_2 layer increases the filling of the valence band many times over. This behavior may be parallel by the enhanced superconducting behavior in terms of the measured value of T_c going from $n=1$ to 4. This observed behavior is similar to that obtained by the Mattheiss.[21]

On the other hand, for the Tl-bilayer systems, the valences of all the atoms remain practically the same, irrespective of the presence of the number of the CuO_2 layers in the system (see Table VII). The Cu valence in the Tl-bilayer systems, in contrast to the behavior seen above for the Tl-monolayer systems, is comparatively smaller and remains constant with the number of CuO_2 layers.

The valences of Ba and O atoms lying in the BaO layer and that of Ca are quite similar in the Tl-monolayer and -bilayer systems and do not reveal any significant variation with the number of layers. In the Tl-monolayer systems, the Tl valence is of the order of 2.4, which is quite high, indicating a bias towards the occurrence of Tl^{+3} in these Tl-monolayer phases. This behavior is quite different from that seen in the Tl-bilayer systems $Tl_2Ba_2Ca_{n-1}Cu_nO_{2n+4}$, where the Tl-valence is seen to be 1.33 because of their low-energy location and high occupation. Here the Tl valence is indicative of the occurrence of Tl^{+1}

The hole concentrations for the various orbitals and the atoms have been computed. For the Tl-monolayer systems, the density of holes is found to be appreciable only for the d levels of Cu and the p levels of O_1, O_2, and O_3 atoms. They are depicted in Table VIII for the various phases. In all the phases, for single atoms, the Cu-d holes dominate over the bonded O-p holes. It may be noted from Table VIII that the hole density per unit cell at Cu atoms increases with the number of CuO_2 layers. This result is in conformity with the observed enhancement of T_c in these systems up to the $n=4$ phases. Further, the present results are in line with the observation of Groen, Leeuw, and Feiner,[23] who have noted an unambiguous relation between T_c and the density of holes per CuO_2 plane for the $n=2$ member of the Bi-based series of superconductors $Bi_2Sr_2Ca_{n-1}Cu_nO_{2n+4}$. In $TlBa_2Ca_{n-1}Cu_nO_{2n+3}$ systems, however, the d-type hole density at the Cu atom per unit cell is high and increases up to $n=6$ phase, although the hole density per CuO_2 does not show a similar behavior.

A perusal of Table IX, which contains the hole concentrations for the Tl-bilayer systems, reveals that, in contrast to the Tl-monolayer systems, more orbitals contribute towards the hole concentrations. Significant contributions arise from the d orbitals of Cu and the p orbitals of all the oxygen atoms. The hole concentration in the Cu-d orbitals and in O-p orbitals enhance approximately in multiples of the number of CuO_2 layers present in the system.

III. SUMMARY AND CONCLUSION

The present tight-binding calculation for the Tl-based systems brings out a number of interesting features in the electronic structure. All the bands have very nearly two-dimensional character. The bands in the neighborhood of the Fermi surface originate mainly from the hybridized Cu($d_{x^2-y^2}$)-$O_1(1)$ [O(2)] orbitals, and some of them either touch E_F or cross it. For the Tl-monolayer systems, the Tl($6s$)-$O_3(p_z)$ antibonding band occurs well above the mixed Cu(d)-O(p) bands throughout the whole Brillouin zone and remains unoccupied. On the other hand, in the case of Tl-bilayer systems, one out of the two Tl($6s$)-$O_3(p_z)$ antibonding bands occurs well above the Fermi surface throughout the Brillouin zone and is thus vacant. The other Tl-O $sp\sigma^*$ band either touches or crosses the E_F. The number of the Cu($d_{x^2-y^2}$)-O($p_{x,y}$) bands crossing E_F is equal to the number of the CuO_2 layers in the phase concerned. All the TlO and BaO layers are seen to be insulating. The CuO_2 layer shows a metallic behavior within its plane and a nearly insulating behavior along the c direction. The present results are in close agreement with those obtained by the LAPW method.[12–14] Also, the calculated DOS for the $Tl_2Ba_2Ca_2Cu_3O_{10}$ phase is in very good agreement with the XPS and IPES data.[22]

For the Tl-monolayer systems, the Cu valence decreases with the number of CuO_2 layers in contrast to Tl-bilayer where it remains constant. The value of $N(E_F)$ in the Tl-bilayer systems increase in multiples of the number of CuO_2 layers present in the system. The Tl valence in the Tl-monolayer systems approaches Tl^{+3} in contrast to the monovalent Tl^{+1} ion in the Tl-bilayer systems. All the cations Ba, Ca, and Tl have quite high valences in comparison to the valence of the Cu cation. The total hole density at Cu atoms in the CuO_2 layers increases with the number of CuO_2 layers, which is in conformity with the observed enhancement of T_c in these phases. The hole concentration in the first member ($n=1$) of the family, $TlBa_2CuO_5$ is comparatively small, a result that is in line with the experimentally observed nonsuperconducting behavior.

ACKNOWLEDGMENT

This work was financially supported by University Grants Commission, New Delhi.

[1]B. Morosin *et al.*, Physica C **60**, 15 (1988).
[2]S. S. P. Parkin *et al.*, Phys. Rev. Lett. **61**, 750 (1988); S. S. P. Parkin *et al.*, Phys. Rev. B **38**, 6531 (1988).
[3]H. Ihara *et al.* Nature (London) **334**, 510 (1988); H. Ihara *et al.*, Phys. Rev. B **38**, 11 952 (1988).
[4]P. Haldae *et al.*, Science **241**, 1198 (1988).
[5]S. Nakajima *et al.*, Physica C **158**, 471 (1989).
[6]T. Manako *et al.*, Physica C **158**, 143 (1989).
[7]H. C. Ku *et al.*, Jpn. J. Appl. Phys. **28**, L923 (1989).
[8]T. Mochiku *et al.*, Jpn. J. Appl. Phys. **28**, L1926 (1989).
[9]M. A. Subramanian *et al.*, Science **242**, 249 (1988).
[10]H. Kusuhara *et al.*, Jpn. J. Appl. Phys. **28**, L1772 (1989).
[11]F. Hentsch *et al.*, Physica C **156**, 485 (1990).
[12]D. R. Hamann and L. F. Mattheis, Phys. Rev. B **38**, 5138 (1988).
[13]V. Kasowski and W. Y. Hsu, Phys. Rev. B **38**, 6470 (1988).
[14]J. Yu *et al.*, Physica C **152**, 273 (1988).
[15]Bal K. Agrawal *et al.*, Bull. Mater. Sci. 14(4) 967 (1991).
[16]Bal. K. Agrawal *et al.*, Phys. Rev. B **45**, 3145 (1992).
[17]Bal. K. Agrawal *et al.*, Physica C **192**, 237 (1992).
[18]Bal K. Agrawal *et al.* (unpublished).
[19]F. Hermann and S. Skillman, *Atomic Structure Calculations* (Prentice Hall, Englewood Cliffs, NJ, 1963).
[20]W. A. Harrison, *Electronic Structure and the Properties of the Solids* (Freeman, San Francisco, 1980).
[21]L. F. Mattheiss, Phys. Rev. B **42**, 10 108 (1990).
[22]H. M. Meyer III *et al.*, Phys. Rev. B **39**, 7343 (1989).
[23]W. A. Groen, D. M. de Leeuw, and L. F. Feiner, Physica C, **165**, 55 (1990).